XVI International Conference on Durability of Building Materials and Components
DBMC 2023, China
K.F. Li and D.P. Fang (Eds)

Tuning the incompatibility between recycled plastic aggregates and cement matrix with polymer-nano silica hybrids

Qiang Zeng[1] **and Ahmed Al-Mansour**[1]

[1]College of Civil Engineering and Architecture, Zhejiang University, 310058 Hangzhou, PR China
cengq14@zju.edu.cn (Qiang Zeng), 11912146@zju.edu.cn (Ahmed Al-Mansour),

Abstract. *Use of recycled waste plastics as the aggregates in construction materials has attracted increasingly gained attention for sustainable construction industry with great environmental benefits. However, the soft plastics and rigid cement matrix can naturally induce the great aggregate-matrix incompatibility, which results in the degradation of engineering properties of cement-based materials containing recycled plastic aggregates (RPAs). To overcome this shortage, this work reports a strategy of tuning the cement matrix with polymer-nano silica (P-nS) hybrids. Ethylene vinyl acetate (EVA) and recycled polypropylene (PP) were selected as the coating polymer and RPA, respectively. Density, strength, water sorptivity and carbonation resistance were measured to assess the physical and mechanical properties of the mortars with recycled PP particles. Microstructure was analyzed using scanning electron microscopy (SEM) with backscattered electron (BSE) and energy-dispersive X-ray spectroscopy (EDS). Results showed that the addition of P-nS hybrids into cement decreases density, mitigates strength reduction, obstructs water sorption, but have positive and negative effects on carbonation resistance of the cement mortars with RPA. The P-nS hybrids build the organic–organic links between the cement matrix and RPA, and coordinate their deformations. The findings of this work proof the proposed strategy of tuning the compatibility between soft aggregates and rigid matrix with the engineered microstructure towards enhancing the recyclability of waste plastics in construction materials.*

Keywords: *Waste plastics; Interfacial transition zones; Water sorptivity; Carbonation resistance; Microstructure.*

1 Introduction

Incessant expansion of population and inhibited urban areas have resulted in aggressive escalation in the consumption of natural resources to build adequate infrastructures. For decades, the construction building material that has been massively utilized the most is concrete, with over 900 Gt accumulated on the Earth (Waters et al., 2016). Because two thirds of concrete is typically natural aggregates, the rising consumption of such resources has negatively reflected in environmental issues due to their needs for preparation and transportation (Mistri et al., 2021). The consumption of concrete and all related production activities have always been accompanied by huge energy consumption that generates CO_2 emissions, sharing over 7% of all carbon footprint blown yearly to the environment(**?**). Therefore, the efforts to obtain environmentally friendly substitutes have been ongoing to acquire more sustainable building materials.

At the same time, the accumulation of plastic waste has become one of the most key environmental problems due to their slow biodegradability, resulting in serious pollution in land and oceans (Kalali et al., 2023). Plastic is used in all aspects of our daily life owing to their excellent properties, light weight, and ease of fabrication, exceeding an annual production amount of 90 billion tons (Hossain et al., 2022). Although most of the plastic types are fully recyclable (**?**),

the recycling rate of plastic does not exceed 10% due to several challenges, such as heterogeneity, contamination, quality degradation, and cost, to name a few. Therefore, plastic waste has been reused as an alternative to other materials to cut back the huge consumption of natural resources and the pollution caused by plastic in the marine and terrestrial ecosystems.

The replacement of natural aggregates by recycled plastic waste has attracted engineers' attention. In fact, the employment of recycled plastic aggregates (RPA) would address both environmental issues, i.e. the huge consumption of natural aggregates and the massive amount of waste plastic.Experimental investigations revealed that concrete with RPA has significantly less weight and potentially greater resistance to impact loads compared with typical concrete (Al-Tayeb et al., 2022). However, the consensus among researchers upon this topic is that the inclusion of RPA in concrete results in a decrease in some of the engineering behaviors, such as workability and strengths. The key reason behind these performance compromises is the weak bond between RPA and cementitious materials due to the smooth surface of plastics. For instance, the direct implementation of RPA in concrete resulted in a strength reduction by up to a quarter when 10% of natural sand was replaced (**?**). Thereof, efforts to lessen the reductions in the engineering properties of RPA concrete applied several physical and chemical treatments for the plastic surface in order to develop stronger bond with the cement matrix. It was found that the interactions of plastics with certain oxidizing chemicals (sodium hydroxide and sodium hypochlorite) could lead to better adhesion between RPA and the cement matrix (**?**). Polymers, on the other hand, have been used to coat plastic surfaces to restrain strength reductions of RPA concrete by enabling stronger interfacial transition zones (ITZs) between RPAs and the cement matrix (**?**Al-Mansour et al., 2022).

Inspired by the reported studies, a novel approach to enhance the engineering properties of RPA cementitious materials is introduced. Polymer-nanosilica (P-nS) hybrids were used to enable efficient upcycling of waste plastic in cement mortar. RPA partially replaced sand by 15 wt%, while EVA and nS were added by weight of cement at 2% $\sim$ 4% and 1% $\sim$ 2%, respectively. All mortars were assessed based on their densities, compressive and flexural strengths, sorptivity performances, and carbonation rates. Sorptivity of the mortars was evaluated by micro-focus X-ray computed tomography (m-XCT), while carbonation was testified using an acid-based indicator and scanning electron microscopy (SEM) with energy-dispersed X-ray spectroscopy (EDS).

2 Materials and sample preparation

2.1 Materials

A Portland cement PI 42.5 (equivalent to ASTM type I) with the clinkers' content over 95% and specific surface area of 355 m^2/kg was adopted as the only inorganic binder to prepare all mortar mixes. A quartz sand with the maximum size of 4 mm was used as the main inorganic aggregate. A type of recycled PP particles with the average size of 2.18 mm and the density of 1.13 g/cm^3 was purchased from Xiamen Keyuan Plastic Co., Ltd. Those PP particles possessed relatively smooth surfaces (**?**). A commercially available redispersible EVA powder with the average size of 571 $\pm$ 29 μm was adopted as the polymeric phase to tune the RPA-matrix incompatibility (**?**). However, pure polymeric EVA would have large shrinkage, so more defects may generate in cement matrix. To further modify the structure of EVA and cement matrix, nano silica (nS)

was added. The average particle size of the nS used was 91 ± 8 μm.

2.2 Sample preparation

A nature sand replacement ratio of 15% and two grades of EVA and nS were designed in this work, so in total, six groups of cement mortar with RPA including the reference group (pure cement mortar) were fabricated (Table 1). The nomenclature was set as follows: Px+Ey+Nz, where P, E and N represent RPA, EVA and nS, respectively, and the symbols x, y, and z denote the content of those materials. A water-to-cement (w/c) ratio of 0.45 was employed for the Ref. mortar. Due to the effects of EVA and nS on workability of cement mortar, w/c ratio was slightly modified to keep the same workability of the mortar slurries (slump of 115 mm).

Table 1. Mix proportions of the mortars with RPA (kg/m^3)

Sample ID	Water	Cement	EVA	nS	Sand	RPA
Ref.	235	525	0.0	0.0	1495	0.0
P15	236	525	0.0	0.0	1450	220
P15E2N1	237	506	10.5	5.3	1450	220
P15E2N2	239	496	10.5	10.5	1450	220
P15E4N1	235	489	21.0	5.3	1450	220
P15E4N2	238	483	21.0	10.5	1450	220

Before mixing, an alkaline solution by dissolving 2 wt% of NaOH into distilled water was created for the enhancement of dispersion of EVA and nS. Later, EVA and nS were added into the alkaline solution followed by high-speed stirrings at 400 rpm for 5 min. After that, RPA particles were added into the readily dispersed EVA and nS suspensions. This step was designed to coat those RPAs with the EVA and nS hybrids. At the same time, a pre-dry mix was performed to the cement and nature sand at 60 rpm for 3 min. Finally, all the materials were mixed together for 3 min to form homogeneous mortar slurries. Cubic and prismatic molds in total of 36 were then filled with the prepared mortar slurries. After sufficient vibrations, the fully filled molds were covered with plastic films to avoid the moisture loss. 24 h later, specimens were demolded and cured in a chamber with the temperature of 22 ± 3 °C and the humidity of 98 ± 2% until testing ages.

2.3 Methods

The bulk cubic/prismatic mortars were used for the tests of density, mechanical properties, water sorptivity and carbonation resistance at 28 d. Density was measured via a high-precision electronic balance for the mortars dried at 60 °C for 24 h. Mechanical properties in terms of compressive and flexural strengths were measured using an INSTRON 8802 full functional servo-hydraulic testing machine. The force control mode at 75 kN/min and the displacement control mode at 1 mm/min were used for compression and flexure tests, respectively. Water sorption of mortar cubes for all six groups was measured by XCT. Generally, the water filled cement-based material can be hardly probed by ordinary industrial XCT because of the low X-ray attenuation of water. To enhance the contract of XCT images of cement-based materials that have been partially filled with water, a solution of cesium iodide (CsI) at the concentration of

25 wt% was adopted as the sorption liquid (**??**). XCT images were reconstructed using CTPro software and the water sorption height was analyzed using VG Studio 3.1. For carbonation tests, some prismatic mortars were first partially sealed with paraffin to allow the occurrence of carbonation in one direction. The specimens were stored in an accelerated carbonation chamber with the humidity of $80 \pm 5\%$, the temperature of 30 ± 3 °C, and CO_2 concentration of $20 \pm 1\%$. The accelerated carbonation lasted for 21 d, then the specimens were split and sprayed with 1% phenolphthalein alcohol solution.

Microstructure of some selected samples was observed via FEI Quanta 650 FEG SEM. Chemical characteristics of local sites in the samples were measured by EDS if necessary. During SEM tests, the acceleration voltage of 20 kV and spot size of 4 were set to acquire the SEM pictures. Samples were oven-dried at 50 oC for 24 h and coated with platinum before SEM tests.

3 Results and discussion

3.1 Physical and mechanical properties

Figure 1(a) shows the density of all bulk mortars. The Ref. mortar had the density of around 2200 kg/m^3. When 15% RPA was blended into the mortar (P15), the density significantly decreased to around 1800 kg/m^3 with the decreasing degrees of 18.2%. This is mainly because RPA (1130 kg/m^3) is much lighter than nature sand (2600 kg/m^3). Further incorporation of EVA and nS into the mortars created minor impacts on density. Compared with P15 mortar, four types of P-nS hybrids only caused the density decreases by $24 \sim 47$ kg/m^3 with the degrees of $1.3\% \sim 2.6\%$. Those slight density decreases are ascribed to the higher air void entrapment in the mortar matrix caused by the EVA polymers (**??**). When more nS was used, the density was slightly increased, owing to the filling effect of nS to polymers. The density values of the mortars with 15% RPA were lower than 1950 kg/m^3, which can be sorted as a type of lightweight concrete material. The data displayed in Figure 1(a) suggest that the partial replacement of nature sand with RPA can be an effective way to decrease the weight of construction materials.

Figure 1(b) displays the compressive and flexural strengths of all mortars. As expected, the Ref. mortar possessed the highest compressive and flexural strengths (35.41 and 4.93 MPa, respectively). When 15% of natural sand was replaced by the recycled PP particles, the compressive and flexural strengths decreased to 28.00 and 3.94 MPa with the decreasing extents of 21% and 20%, respectively. When the P-nS hybrids were mixed in the mortars, strengths rose slightly. Specifically, the addition of 2% EVA and 1% nS into the mortar with 15% RPA (P15E2N1) caused the increase of compressive strength by 2.3%, but almost no changes to the flexural strength. Further increase of either EVA or nS promoted the strengths in very limited extents (less than 4%). The results of Figure 1(b) suggest that the P-nS hybrids may have no significant effect on the mechanical properties. The observations are reasonable, because the single addition of either polymers or RPA (or their combination) into cement mortar would cause obvious strength decreases (**?**). Our data at least testified that the P-nS hybrids can cease the decrease of strength of cement-based material with polymers.

However, if one determined the strength-to-density (SD) ratio, different trends appeared. Generally, materials possess positive correlations between density and strength, that is, a material with higher density also has higher strength (**?**). This strength-density law governs the

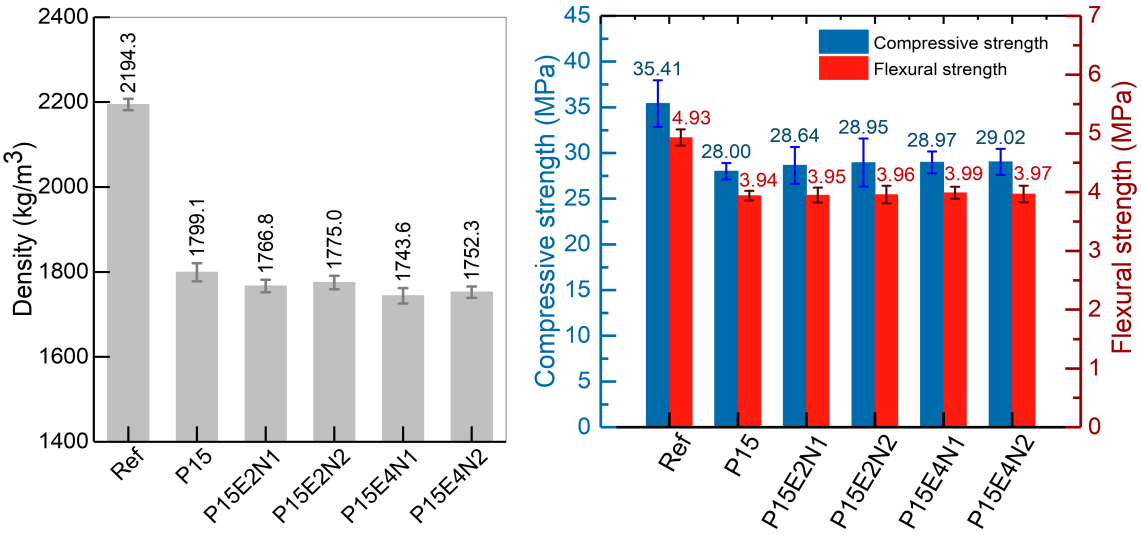

(a) Density (b) Strength

Figure 1. Density and strength of all bulk mortars.

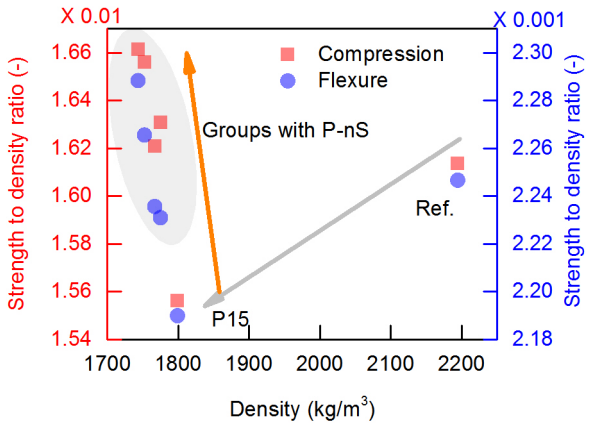

Figure 2. Strength-to-density (SD) ratio of all mortars.

results of samples Ref. and P15 (Figure 2). For the RPA mortars with P-nS hybrids, an opposite trend was found. Specifically, the SD ratio increased from 1.556% for P15 mortar to 1.662% for P15E4N2, as the density decreased from 1800 to 1744 kg/m^3. Similar trends were found in the SD ratios from the flexural tests (Figure 2). The sharp increase of SD ratio for the P-nS groups suggests that the P-nS additives may establish more porous structure with stronger skeletons.

3.2 Durability

To assess durability of the cement mortars with RPA and P-nS hybrids, water sorption and carbonation resistance were measured. The water sorption height in cubic mortar specimens was probed by XCT with the contract enhancing agent of CsCl at 25wt% (see Figure 3a for the testing flowchart). Figure 3b displays the sorption heights in the mortars after 540 min. Clearly, the bottom part of the mortars showed a higher brightness, because much severer X-ray attenuation took place when the X-ray beams penetrated the mortars filled with the CsCl solution (**?**). In this regime, the water penetration fronts were marked in the figures that enable separation between the CsI-filled and unfilled zones in the mortar matrix.

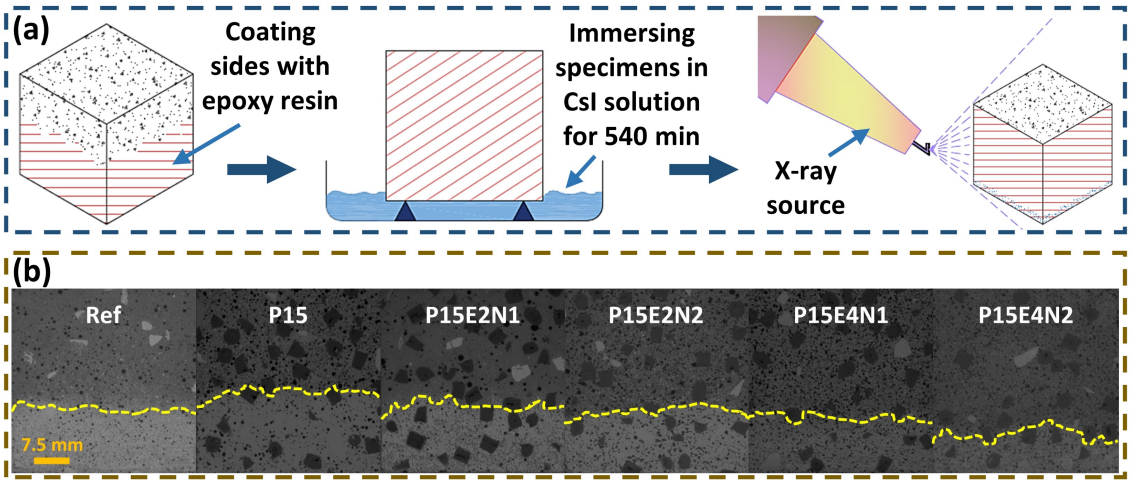

Figure 3. Sorptivity of the mortars: (a) flowchart of XCT tests with the contract enhancing agent of CsCl (25% mass concentration), (b) sorption heights and fronts of the mortars at 540 min.

For the Ref. mortar, the liquid penetration height was around 15 mm, while that of the P15 mortar was lightly higher (up to 18 mm). For the mortars with both the RPA and P-nS additives, the liquid penetration heights were significantly decreased. The liquid penetration heights of mortars P15E2N1, P15E2N2, P15E4N1 and P15E4N2 were 14.5, 13, 11 and 8.5 mm respectively. The nearly half decreases of liquid sorption height for the P15E4N2 mortar compared with the Ref. mortar is mainly due to the obstructing effect of polymers that can fill the open channels and the ITZs between cement matrix and aggregates, as well as decrease hydrophility of the pores (**?**). One may also notice some dark polygons in the XCT images that represent the recycled PP particles with relatively low X-ray attenuation (Figure 3(b)). It seemed that more PA particles appeared on the top half of P15, while relatively homogeneous RPA distributions were found in the P-nS groups (Figure 3b). Those can be due to the fact that nano particles

and polymers can enhance the viscosity of cement slurries (**?**), so the light PP particles can be maintained in the mortar with time.

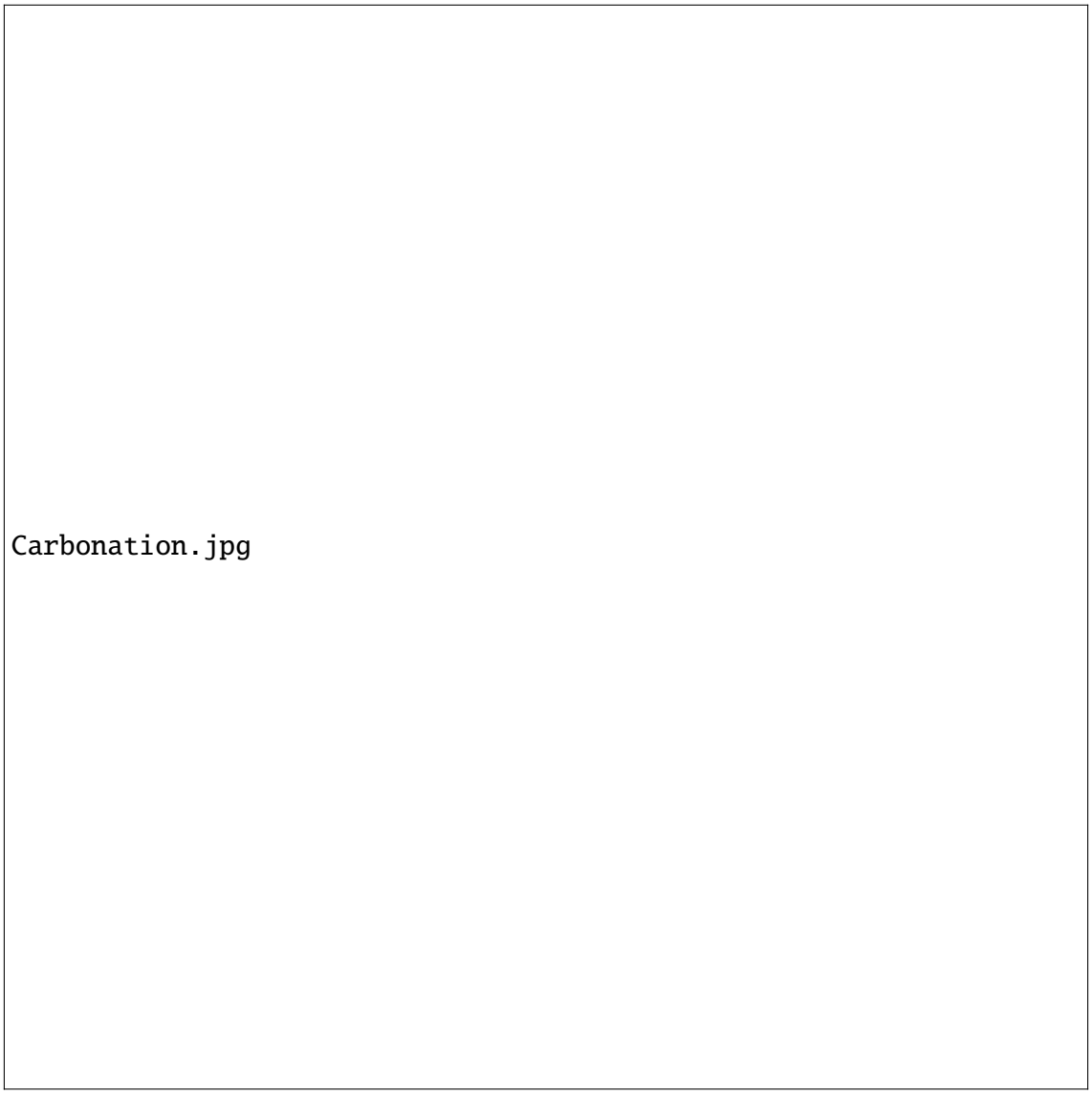

Figure 4. Color of the fractured mortar surfaces with phenolphthalein and the measured carbonation depths.

The carbonation resistance results of the mortars are shown in Figure 4. At a first glance, only the surface part of the mortars has been carbonated for 21 d. The Ref. mortar had the carbonation depth of around 7.7 mm, while the P15 mortar showed a deeper carbonation depth of around 9.1 mm. The severer carbonation of the P15 mortar can be caused by the more porous ITZ between the PP aggregates and cement matrix (**?**). When the P-nS hybrids were incorporated into the cement mortars, complex phenomena appeared. At the low EVA dosages (2%), P15E2N1 and P15E2N2 showed the carbonation depths of 6.6 and 4.3 mm, respectively, greatly lower than that of P15. However, when the EVA dosage was increased to 4%, a deeper carbonation was measured for P15E4N1 with the carbonation depth of 10.2 m, and the mitigation effect

on carbonation was depressed for P15E2N2 with the carbonation depth of 7.1 mm (Figure 4). Those can be because the polymerization of EVA in high dosages with cement hydration would introduce more polymer pores into cement matrix (**?**), which would have more effective obstruction to water penetration, but less to gas transport. It is interesting to note that the carbonated areas in the P-nS modified RPA mortars showed lighter red color than those in the Ref. mortar (Figure 4). The regime is that polymers can retard cement hydration, so less calcium hydroxide (CH) is formed (**?**).

3.3 Microstructure and mechanisms discussion

Figure 5 selectively demonstrates the BSE images of P15, P15E2N2, and P15E4N2 samples. Since focus was mainly put on the cement matrix-RPA incompatibility, BSE tests were therefore conducted to measure the ITZs between PP aggregates and cement matrices. In the BSE images, the dark phases represent plastics, where the bright ellipses and/or needles in the recycled PP aggregates denote glass fibers, which are used as the reinforcement when recycling the plastics. The sharp contrasts and different textures among the PP particles, sand and cement matrices allowed us to easily identify those phases. Apparently, the cement matrices had tight contact with both the PP and sand particles (Figure 5). For the cement matrices, the sample with higher EVA content showed darker color, owning to the fact that incorporation of EVA into cement can greatly decrease material's density (Al-Mansour et al., 2022). Meanwhile, polymer clusters can form in the cement matrix, so the organic-organic adhesion can be built between the RPAs and polymers. Less incompatibility and stronger adhesion between the RPA and cement matrix are thus expected.

To better understand the differences in microsturcture between different phases, EDS line scans were performed in local areas. Data of P15 demonstrated that when EDS scans performed from point A to B in Figure 5a1, content of C in the PP aggregate decreased heavily to near zero, while those of O, Si and Ca increased greatly (Figure 5a2). For P15E2N2, C was probed in cement matrix (or ITZ) near the PP aggregate, suggesting the agglomeration of P-nS particles on the PP surfaces. The agglomeration thickness was around 25 μm (Figure 5b2). For P15E4N2, C was detected in much broader areas (Figure 5c2), owing to the fact that more EVA polymers were blended into the cement matrix. The gray particles were sand as evidenced by only signals of Si and O (Figure 5c2).

Micro morphology of the selected carbonated areas in P15, P15E2N2, and P15E4N2 was observed via SEM. Since carbonation would have no impacts on sand and RPA particles, focuses were put on the micro morphology of cement matrices. As can be seen in Figure 6, the cement matrix of P15 sample showed a porous structure (Figure 6a1 and a2) with large $CaCO_3$ polymorphism (Figure 6a)). For P15E2N2 and P15E4N2 samples, the matrices were relatively denser (Figure 6b1, b2, c1 and c2), so the strengths were slightly higher (Figure 1). EVA polymers that showed as a smooth phase were observed in both P15E2N2 and P15E4N2 samples (Figure 6b3 and c3).

From both ITZ and microstructure tests, all phases including sand, RAP and cement matrix can be tightly adhered together to form bulk cement mortars. However, the strength data indicated that 15% replacement of nature sand by the PP particles caused the decreases in density by 18% and compressive strength by 20% (Figure 1). The regimes may include:

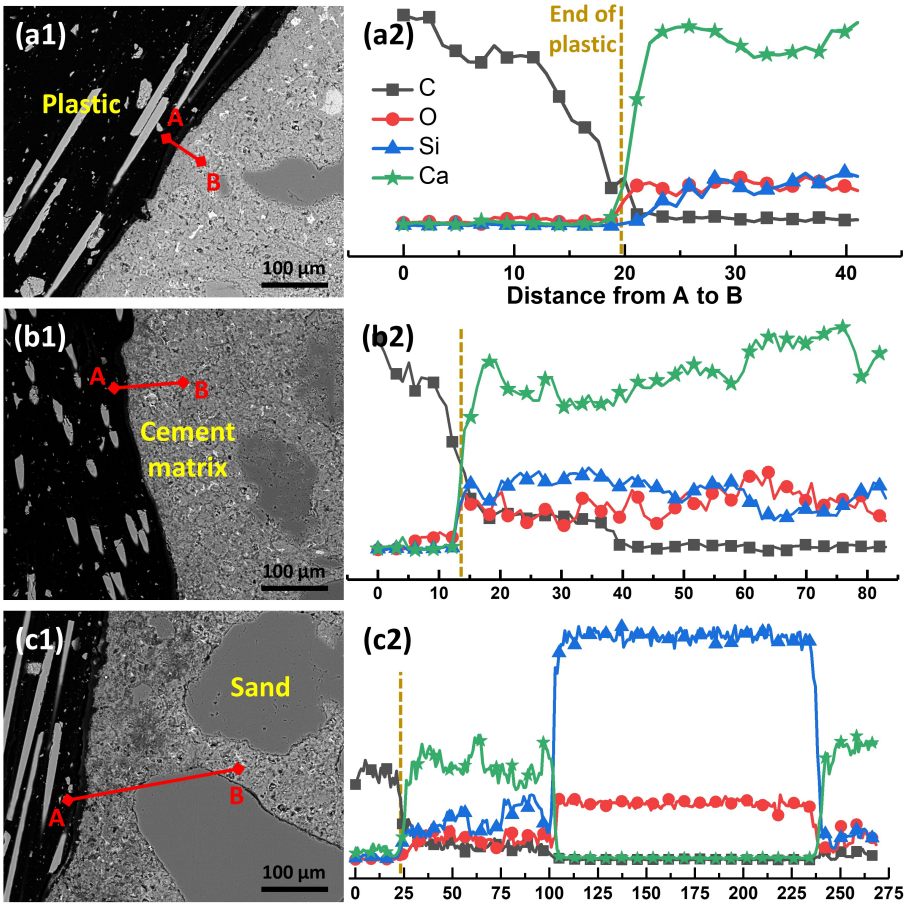

Figure 5. ITZ measurements of (a) P15, (b) P15E2N2, and (c) P15E4N2; left column: BSE images; right column: element distributions of C, O, Si and Ca by EDS scans from A to B marked in panels (a1) to (a3).

a) strength of the recycled PP is lower than that of nature sand;
b) plastic particles are more hydrophobic than nature sand, so the PP-cement adhesion would be weaker than the sand-cement one;
c) the intrinsic mechanical properties of the recycled PP, such as elastic modulus, shear modulus and Poison ratio, are different from those of nature sand, so the deformation of the RPA aggregates is not consistent with that of the cement matrix under external loading.

Those aspects suggest that RPA has worse compatibility with cement matrix than nature sand. To tune the aggregate-matrix compatibility, a type of P-nS additive was added into cement to lower brittleness of the cement matrix. On the one hand, EVA polymers can form nano-sized pores in cement hydrates (**?**), so the density can be further slightly reduced, and the deformability of the polymer-modified cement matrix can be substantially increased. On the other hand, the filling effect of nS in EVA and cement matrix can enhance their strength, therefore the bulk strength can be maintained or slightly enhanced for the P-nS modified mortars (Figure 1).

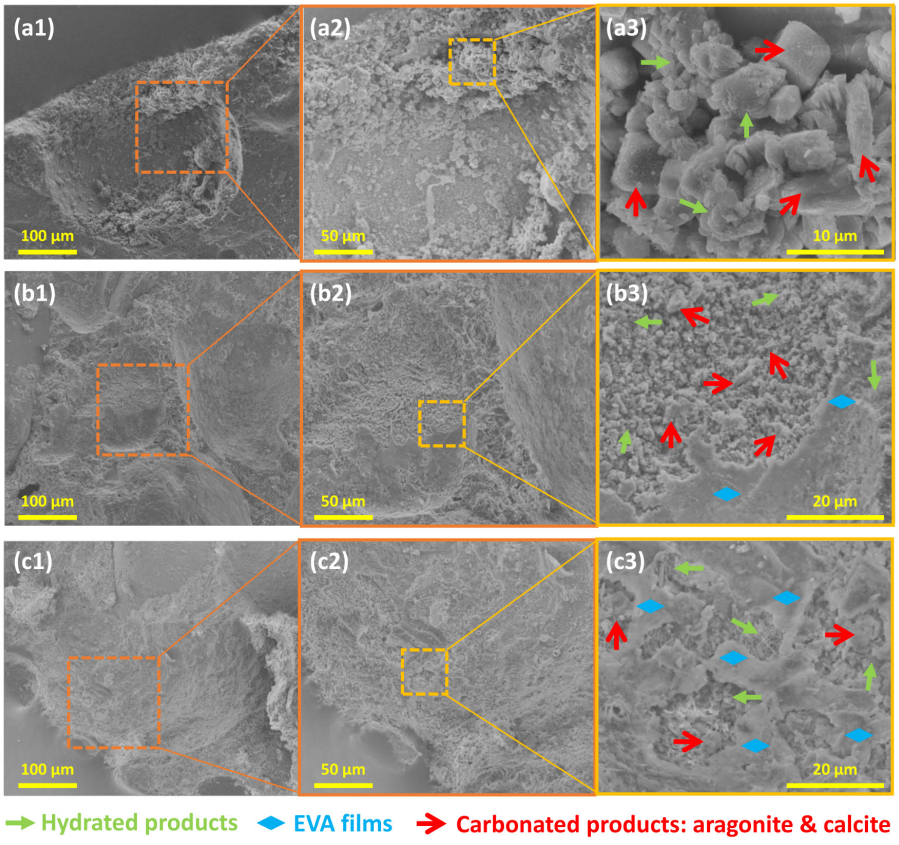

Figure 6. SEM images of selected carbonated areas of (a) P15, (b) P15E2N2, and (c) P15E4N2; left to right columns: low to high magnifications.

Polymers generally form impermeable films in cement matrix and retard cement hydration (**??**), so the water resistance was substantially increased (Figure 3). The regimes can also enhance the carbonation resistance to some extent, e.g., for samples P15E2N1 and P15E2N2.

However, high dosages of polymers may cause more nano pores that enable migration of gas molecules, so the carbonation resistance was decreased, e.g., for sample P15E4N1 (Figure 4).

4 Conclusions

- Replacement of nature sand with 15wt% RPA substantially decreases the density and strengths by 18% and 20% respectively. Further incorporation of the hybrid P-nS additives can slightly reduce the density but raise or maintain the strengths. This causes an opposite trend to the traditional positive strength-density correlations.
- The sole RPA replacement slightly enhances water sorption due to the more porous RPA-matrix ITZs. The integrated RPA replacement and hybrid P-nS additives can obviously decrease water sorption due to the pore blockage effect of polymers. The regimes also partially account for the enhancement of carbonation resistance for the mortars with 2% EVA. The more porous structure of cement mortar with high dosages of EVA would depress the carbonation resistance.
- PP, sand and cement matrix can be clearly identified in BSE images, and all the phases show relatively tight adhesion. Polymer clusters can build organic-organic adhesion and decrease the rigidity of cement matrix, therefore the RPA-matrix compatibility is enhanced.

Acknowledgements

The authors greatly thank the financial support from the National Natural Science Foundation of China (No. 52038004) and ZJU-ZCCC Institute of Collaborative Innovation (No.ZDJG2021008).

ORCID

Qiang Zeng: https://orcid.org/0000-0003-1720-4766
Ahmed Al-Mansour: https://orcid.org/0000-0002-3048-5841

References

Al-Mansour, A., Chen, S., Xu, C., Peng, Y., Wang, J., Ruan, S., & Zeng, Q. (2022). Sustainable cement mortar with recycled plastics enabled by the matrix-aggregate compatibility improvement. *Construction and Building Materials*, *318*, 125994.

Al-Mansour, A., Dai, Y., Xu, C., Yang, R., Lu, J., Peng, Y., ... Zeng, Q. (2023). Upcycling waste plastics to fabricate lightweight, waterproof, and carbonation resistant cementitious materials with polymer-nano silica hybrids. *Materials Today Sustainability*, *21*, 100325.

Al-Mansour, A., Yang, R., Xu, C., Dai, Y., Peng, Y., Wang, J., ... Xu, S. (2022). Enhanced recyclability of waste plastics for waterproof cementitious composites with polymer-nanosilica hybrids. *Materials Design*, *224*, 111338.

Al-Tayeb, M. M., Aisheh, Y. I. A., Qaidi, S. M. A., & Tayeh, B. A. (2022). Experimental and simulation study on the impact resistance of concrete to replace high amounts of fine aggregate with plastic waste. *CASE STUDIES IN CONSTRUCTION MATERIALS*, *17*.

Hasanbeigi, A., Price, L., & Lin, E. (2012). Emerging energy-efficiency and co2 emission-reduction technologies for cement and concrete production: A technical review. *RENEWABLE & SUSTAINABLE ENERGY REVIEWS*, *16*(8), 6220-6238.

Hossain, R., Islam, M. T., Ghose, A., & Sahajwalla, V. (2022). Full circle: Challenges and prospects for plastic waste management in australia to achieve circular economy. *Journal of Cleaner Production*, *368*, 133127.

Islam, J., Shahjalal, M., & Haque, N. M. A. (2022). Mechanical and durability properties of concrete with recycled polypropylene waste plastic as a partial replacement of coarse aggregate. *JOURNAL OF BUILDING*

ENGINEERING, *54*.

Kalali, E. N., Lotfian, S., Shabestari, M. E., Khayatzadeh, S., Zhao, C., & Nezhad, H. Y. (2023). A critical review of the current progress of plastic waste recycling technology in structural materials. *CURRENT OPINION IN GREEN AND SUSTAINABLE CHEMISTRY*, *40*.

Mistri, A., Dhami, N., Bhattacharyya, S. K., Barai, S., V, Mukherjee, A., & Biswas, W. K. (2021). Environmental implications of the use of bio-cement treated recycled aggregate in concrete. *RESOURCES CONSERVATION AND RECYCLING*, *167*.

Ouyang, J., Han, B., Chen, G., Zhao, L., & Ou, J. (2018). A viscosity prediction model for cement paste with nano-sio2 particles. *Construction and Building Materials*, *185*, 293-301.

Peng, Y., Zeng, Q., Xu, S., Zhao, G., Wang, P., & Liu, X. (2020). Bse-ia reveals retardation mechanisms of polymer powders on cement hydration. *Journal of the American Ceramic Society*, *103*(5), 3373-3389.

Peng, Y., Zhao, G., Qi, Y., & Zeng, Q. (2020). In-situ assessment of the water-penetration resistance of polymer modified cement mortars by μ-xct, sem and eds. *Cement and Concrete Composites*, *114*, 103821.

Thorneycroft, J., Orr, J., Savoikar, P., & Ball, R. J. (2018). Performance of structural concrete with recycled plastic waste as a partial replacement for sand. *CONSTRUCTION AND BUILDING MATERIALS*, *161*, 63-69.

Waters, C. N., Zalasiewicz, J., Summerhayes, C., Barnosky, A. D., Poirier, C., Galuszka, A., ... Wolfe, A. P. (2016). The anthropocene is functionally and stratigraphically distinct from the holocene. *Science*, *351*(6269), aad2622.

Zeng, Q., Lin, Z., Zhou, C., & Wang, J. (2019). Capillary imbibition of ethanol in cement paste traced by x-ray computed tomography with cscl-enhancing technique. *Chemical Physics Letters*, *726*, 117-123.

Zeng, Q., Wang, X., Yang, R., Jike, N., Peng, Y., Wang, J., ... Yan, D. (2021). Transmission micro-focus x-ray radiographic measurements towards in-situ tracing capillary imbibition fronts and paths in ultra-thin concrete slices. *Measurement*, *175*, 109141.

Zhao, K., Zhao, L., Hou, J., Zhang, X., Feng, Z., & Yang, S. (2021). Effect of vibratory mixing on the slump, compressive strength, and density of concrete with the different mix proportions. *Journal of Materials Research and Technology*, *15*, 4208-4219.